Improvement Of Syngas Quality In Fixed Bed Gasifier Using Camg(CO₃)₂ Catalyst

**Darshit S Upadhyay[1*], Amita Chaudhary[2], Akshit Trada[1], Dhruvil Patel[1], Rajesh N Patel[1]**
[1]Mechanical Engineering Department, Institute of Technology,
Nirma University, Ahmedabad
*Corresponding Author, darshitupadhyay@yahoo.com, +91 9428966766
[2]Chemical Engineering Department, Institute of Technology, Nirma University, Ahmedabad
amita.chaudhary@nirmauni.ac.in

Abstract - This paper deals with the experimental investigation of lignite (L) and wood (W) feedstock in a pilot-scale downdraft gasifier. The study aims to check the compatibility of $CaMg(CO_3)_2$ [dolomite (D)] catalyst, 5% (W/W), with lignite and wood (L+D, W+D) feedstock as an additive to enhance the performance of a 10 kWe atmospheric pressure downdraft gasifier system. Fuel consumption and gas flow rate were found to be 10.01-11.6 kg h^{-1} and 26.76-29.57 kg h^{-1}, respectively, for lignite and wood feedstock (with and without catalyst). In lignite, CO and H_2 concentrations were increased by 6.81 % and 4.9 %, respectively, whereas in wood, their concentrations were increased by 8.88 % and 5.1 % when the catalyst was employed with feedstock. The producer gas LHV and cold gas efficiency were increased by 6.02% and 5.75% in lignite and 6.97% and 6.61 in wood, whereas specific fuel consumption decreased by 5.92% (in L), 5.17 (in W) with dolomite feedstock. Tar and Total Particulate Matter (PM) concentrations in the producer gas were measured and found to have a noticeable decline with catalytic gasification for both feedstocks. The study concludes that adding dolomite offered better results in terms of higher efficiency and lower tar–PM concentrations.

Graphical Abstract:
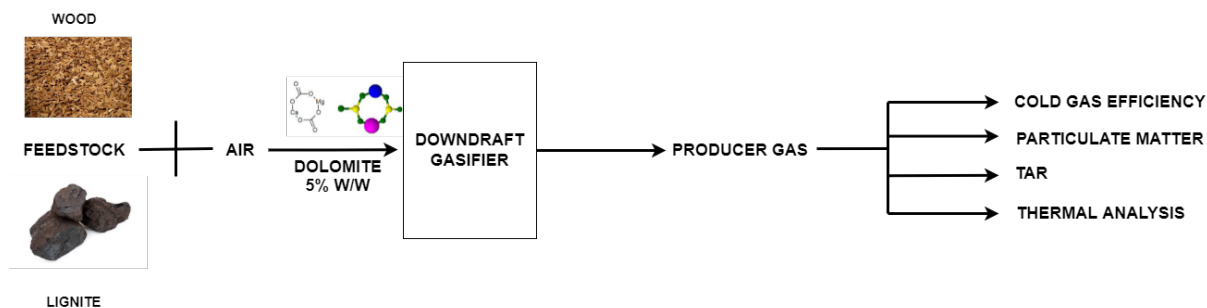
Keywords: Catalyst, Gasifier, Lignite, Cold Gas Efficiency, Thermodynamic analysis

Abbreviation:

η	Energy efficiency	FC	Fixed Carbon
β	correlation factor	GC/MS	Gas chromatography–Mass spectrometry
ψ	Exergy efficiency	GHE	Greenhouse emissions
A,B,C,D,E	specific heat constant	H	Hydrogen
C	Carbon	H_2	Hydrogen gas
CH_4	Methane	H_2%	Mass fraction of hydrogen
CH_4%	Mass fraction of methane	HHV	High Heating Value
CO	Carbon monoxide	LHV	Lower Heating Value (MJ kg^{-1})
CO%	Mass fraction of carbon monoxide	MBC	Mass balance closure
CO_2	Carbon dioxide	MC	Moisture content

$CO_2\%$	Mass fraction of carbon dioxide	MJ	Mega Joule
$C_{p, feed}$	Average specific heat of feed	N	Nitrogen
DSC	Differential Scanning Calorimetry	$N_2\%$	Mass fraction of nitrogen
EBC	Energy balance closure	O	Oxygen
E^{ch}	chemical energy	PM	Total Particulate Matter
E^{ph}	Physical energy	R	Gas constant
E_x	Exergy	T_0	Ambient Temperature
$E_x BC$	Exergy balance closure	TGA	Thermal gravimetric analysis
E_x^{Ch}	Chemical exergy	VM	Volatile Matter
E_x^{Ph}	Physical exergy		

1. Introduction

Cleaner power and electricity generation can be achieved by utilizing renewable and long-lasting energy sources such as wind, solar and biomass. In the technology and construction sector, biomass in the form of forestry wastes and agricultural residues offers a lot of potential for substantial energy production. Electrical energy, for example, is widely used in rural and urban regions for home, agricultural, and industrial purposes [1]. The current study focuses on energy generation from these resources to meet energy demands, particularly in rural regions, due to the wide and diversified regional biomass availability [2]. Biomass gasification is a thermochemical conversion process that converts biomass into producer gas. It is rich in CO and H_2 and has a lower/medium heating value. This gas can be used for thermal power and electricity generation. Gasification generates producer gas by partially burning biomass under low oxygen (sub-stoichiometric) conditions. The major constituents of producer gas are H_2, CO, and CH_4, with traces of CO_2 and N_2. The leftover products of this gasification procedure include tar and ash. Gasification is one of the most effective ways to remediate low-quality feedstock. Generally, high-temperature slagging gasifiers perform best with high-rank, less reactive coals, whereas dry-feed gasifiers function well with low variety, high moisture coals. [1]. Higher ash and silicates in a feedstock (such as lignite) create clinkers which are responsible for interruption in continuous gasification operation [2], [3]. To overcome such a problem, researchers suggested different options such as co-gasification of feedstock [4], manipulating grate movement and changing air feed position [5], additional suitable catalyst [6], etc.

Tar and Total Particulate Matter (PM) are the major producer gas contaminants [7]. If the concentrations of such contaminants are higher, they create unacceptable maintenance downstream of the system [8]. Different methods to diminish Tar and PM include physical, non-catalytic, and catalytic processes. The catalytic approach is preferred over other methods due to its potential to boost conversion efficiency along with reducing pollutants. This procedure primarily entails tar removal, which involves a high-temperature reaction between hot gas and the catalyst. This approach chemically converts tar into light fraction gases [9]. Researchers used different catalysts such as clay minerals, calcined rocks, char, olivine, FCC (Fluid Catalytic Cracking), activated alumina, alkali metal-based, iron ores, transition metal-based catalysts, and other transition metal oxides.

Calcium oxide (CaO) is a relatively inexpensive ingredient (found in limestone or dolomite) that aids in the breakdown of tar compositions. Upadhyay et al. [6] experimented on a 10 kWe downdraft gasifier by varying the catalyst to lignite (C/L) ratio to investigate the clinker formation and gasifier performance. They observed that clinker formation was almost negligent, and tar – PM concentrations were within permissible limits at a 7% $MgCO_3$ C/L ratio. In further studies, it was also investigated that the H_2/CO ratio, gas yield, CGE, LHV, and exergy efficiency also improved by 9.94%, 2.52%, 20.24%, 22.22%, and 29.04%, respectively, with the same ratio when the catalyst was employed to the reactor. Chen et al. [9] employed Ni-loaded steel slag as a catalyst, which is high in metal oxides, to optimize syngas quality for sludge steam gasification. A catalyst loading of 20%, a steam flow rate of 1.0 g min $^{-1}$, and a temperature of 900°C was the most effective condition for producing high-quality hydrogen-rich syngas. Zeng et al. [10] performed experiments on two-stage alkaline thermal gasification of cellulose with $Ca(OH)_2$ sorbent and catalytic reforming with Ni/Fe dual-functional CaO-based catalysts. They achieved H_2 yield (27.36 mmol g^{-1} cellulose), H_2 concentration (79.22 v%), and H_2 conversion (57.61%) at a 500 °C temperature. The literature shows that there is a huge scope in the catalytic gasification process, especially in improving the quality of producer gas and reducing clinker formation.

This paper deals with the experimental study of a gasification system with lignite and wood as fuels and dolomite as a catalyst. To check the compatibility of a catalyst with feedstock, the addition of 5% dolomite with lignite was selected

based on the literature review. Gasifier performance, such as fuel flow rate, air-gas flow rate, producer gas concentration, cold gas efficiency, specific fuel consumption, tar, and PM in the producer gas, was measured for wood and lignite with and without using a catalyst. Thermodynamic analyses such as mass, energy, and exergy balance are also conducted in this study.

2. Materials and Methodology
2.1. Fuel

Table 1. Characterization of wood and lignite.

Analysis	Wood	Lignite
Proximate Analysis		
Volatile Matter	73.40	42.09
Moisture	6.70	11.77
Ash	5.20	15.07
Fixed Carbon[a]	14.70	31.07
Ultimate Analysis		
Carbon	40.30	37.78
Hydrogen	5.37	4.95
Sulphur	0.008	0.141
Nitrogen	1.28	1.559
Oxygen[a]	46.35	40.50
Bulk Density (kg m^{-3})	526	776
Heating Value (MJ kg^{-1})	18.24	16.37
Particle size (mm)	25*25*25	22-25

[a] By difference

Lignite and scrap wood (Tectona grandis, teak wood) were selected as feedstock for the experimentation in the 10 kWe downdraft gasification system. Lignite and wood were procured from Rajpardi lignite mines (Gujarat, India) and a neighbouring furniture workshop. As reported earlier, lignite was crushed and screened to get in the desired size (22-25 mm) [2]. Wood was cut from a woodcutter in 25*25*25 mm size. The heating value, particle size, ultimate and proximate analysis and bulk density of lignite and wood were measured and mentioned in Table 1. Proximate and ultimate analysis was carried out with Leco TGA 701 (Test method: IS 1350 (Part I)-1984) and Leco ThuSpec CHNS (Dry basis). A digital bomb calorimeter (Instrument: Leco AC-350, Part II)-1970, Test method: IS 1350) was used to measure the heating values of the feedstock. Plastic air-tight containers were used to store the feedstock to preserve its composition and qualities throughout storage.

2.2. Catalyst

Dolomite CaMg(CO$_3$)$_2$ was used as a catalyst for this study. Lump dolomite was taken from Udaipur (Rajasthan, India) in a natural form. It was broken and sieved to maintain particle size between 22-25 mm. Dolomite was added with the lignite or wood feedstock (5%, W/W) for experimentation. Dolomite was characterised to identify its behaviour with feedstock during the gasification process.

2.2.1 XRF (X-ray fluorescence) Analysis

A solid dolomite and lignite ash sample is irradiated with high-energy X-rays from a controlled X-ray tube. A standard instrument, Rigaku X-Ray Spectrometer: Model-ZSX mini-II, is used to analyse dolomite Lumps (22-25 mm). The identification of major, minor, and accessory minerals in oxide states and their percentage is tabulated in Table 2.

The main constituents present in the dolomite lumps are CaO (48.67%) and MgO (27.77%), as mentioned in Table 2. As a result, this is believed to be pure dolomite. Several elements with 13 % content also had Al_2O_3, SiO_2, Cr_2O_3, and Fe_2O_3.

Table 2. XRF composition of dolomite and lignite ash (in %)

Contents	Dolomite lump	Lignite Ash
MgO	27.7705	2.627
Al_2O_3	3.2825	9.664
SiO_2	9.7760	17.676
K_2O	0.1005	0.126
CaO	48.6779	32.49
Cr_2O_3	3.5979	0.167
MnO	0.2607	0.994
Fe_2O_3	6.2730	21.286
NiO	0.2609	0.026
SO_3	-	12.375

2.2.2 XRD (X-ray diffraction) Analysis

The crystalline structure of dolomite lumps was characterized by the XRD technique in a Philips X'PERT MPD X-ray diffractometer (UC Santa Barbara), with a source of Cu Kα (1.5405 Å). After various treatments, the XRD patterns of the calcined sample were recorded in a 2θ range between 10⁰ and 80⁰, with a rate of 4⁰/min. In the XRD analysis, the data were collected from 0 to 80 2θ. The highest peak was seen at 2θ 30⁰of calcite ($CaCO_3$). These Sharp peaks of dolomite appear on 2θ 30.934⁰ and 41.108⁰ are resembled with rhombohedral crystal system, as shown in Fig. 1. The obtained XRD of dolomite lumps was compared with the standard XRD of fresh dolomite. The weight % of calcium and magnesium oxide varies based on the dolomite source, and the weight % of calcium and magnesium oxide was a key determinant of dolomite effectiveness. The tar cracking efficiency was lowest in dolomites with lower CaO and MgO composition.
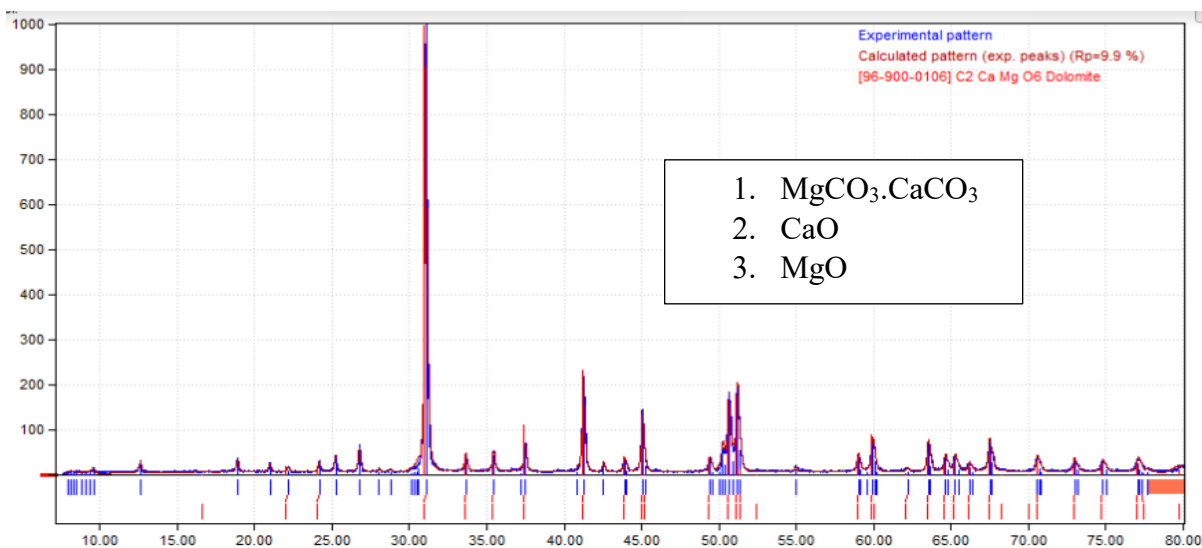

Fig. 1. XRD analysis of dolomite lump

3. Experimental and Thermodynamic analysis

3.1 Experimental setup

The experiments were conducted in a 10 kWe atmospheric pressure downdraft gasifier with wood and lignite as fuel and dolomite lump as a catalyst. A representation of the gasification system diagram is illustrated in Fig. 2. A vibration apparatus was mounted at the top side of the gasifier reactor to prevent the fuels from channelling or bridging inside the reactor. The water circulating pump, water tank, and water jet (nozzle) arrangement provided negative pressure for smooth gas flow. A wet scrubber, surge tank (sawdust-filled), and fabric filter were kept downstream of the gasifier to get a dust-free gas. The gas flow was observed using a calibrated orifice meter (with a U-tube manometer), and temperatures were measured using calibrated thermocouples (K type, Chromel-Alumel). Thermocouples were used to measure temperatures in the vertical direction inside the gasifier reactor in this investigation. A hotwire anemometer (Amprobe TMA-21HW) with a data logger and a Shimadzu 2010 gas chromatograph was used to evaluate air flow rate and producer gas concentrations, respectively. A Shin Carbon ST 100/120 micro-packed column and micro-thermal conductivity detector were used in a gas chromatograph. After the cold start, a flame is attained at the gas burner (15-20 min). The temperatures in the gasifier did not change significantly after the flame propagated. The experiments were conducted three times to check the repeatability of the results.

#		#	
1	Top Cover	9	Water Tank
2	Main Body	10	Water Pump
3	Vibrating Mechanism	11	Gas Burner
4	Air Nozzle	12	Sawdust Filled Surge Tank
5	Thermocouple	13	Fabric Filter
6	Ash Removal	14	Particulate Filter Holder with Controller
7	Cyclone Saperator	15	Shell and Tube Type Glass Condenser
8	Water Jet Nozzel	16	Vacuum Pump

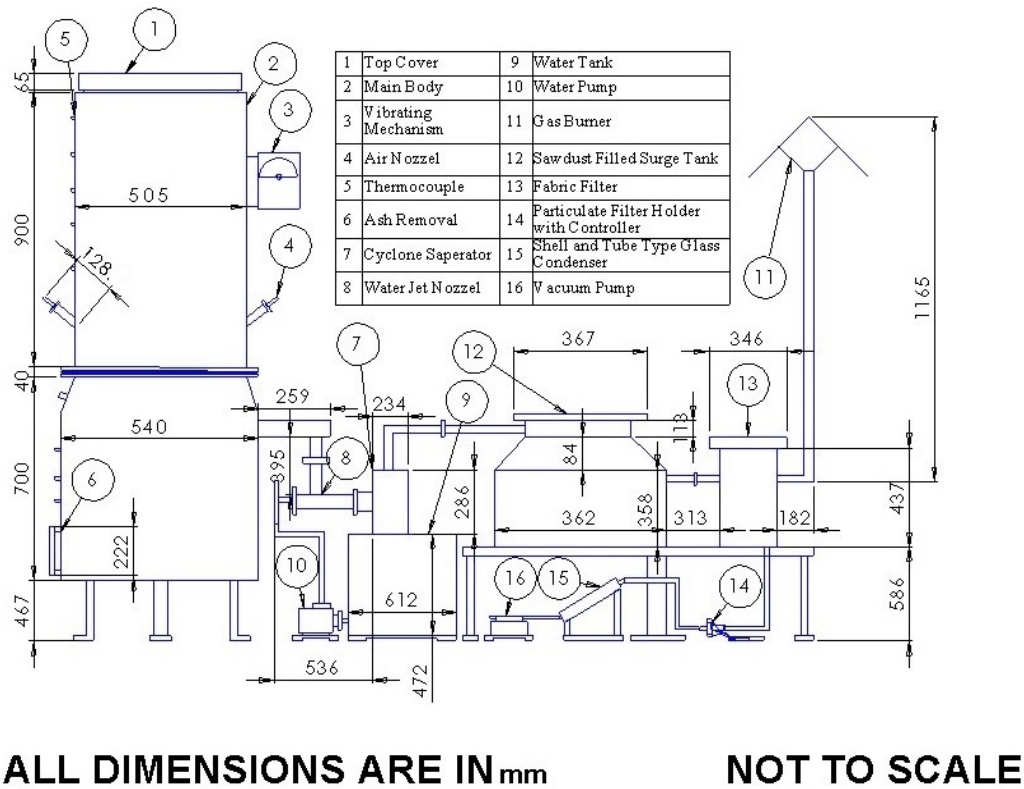**ALL DIMENSIONS ARE IN mm   NOT TO SCALE**

Fig. 2. Schematic diagram of downdraft gasification system [6]

Total Particulate Matter (PM) and tar were measured as per the standard of the Ministry of New and Renewable Energy (MNRE), Government of India [11]. A setup was developed for measuring these contaminants: a PM holder with mica heater, shell and tube type glass condenser, chilling water arrangement with circulating pump and vacuum pump. Axiva makes glass fibre filter paper was used for collecting total particulate matter. The producer gas stream was taken from the mainline and diverted the producer gas in this system through a vacuum pump. The detailed working of the gasification system and tar-PM measurement can be found in the authors' previous work [2], [6], [8], [12].

3.2 Thermodynamic Analysis

3.2.1 Mass Balance

This study aimed to conduct a mass balance analysis to determine the reliability of all the experiments conducted on the gasification of various feedstocks in the 10kWe gasifier. Mass conservation must hold for a control volume, i.e., the difference between input and output masses must equal zero. The feedstock and atmospheric air comprise the entire input mass, while the dry producer gas, char, tar, ash, and water vapours comprise the total output mass. Tar production was found insignificant in contrast to all other masses; thus, it was removed from the analysis [4].

For the gasification process, the following mass balance equation was used:

$$m_{feed} + m_{air} = m_{gas} + m_{tar} + m_{char} + m_{water} + m_{ash} \tag{1}$$

The m_{feed} and m_{air} in the above equation represents the mass consumption rate of feedstock and mass flow rate of oxidizer in gasifier respectively while m_{gas}, m_{ash}, m_{char}, m_{tar} and m_{water} represent the mass flow rate of producer gas, ash, char, tar, and water formed in the process, respectively.

3.2.2 Energy Balance

For any thermal system, studying energy balance is critical since it can assist in reducing system losses. It is a crucial thermodynamic study that aids in improving the system's performance. The equation was used to calculate the energy balance.

$$E_{feed} + E_{air} = E_{gas} + E_{char} + E_{ash} + E_{tar} + E_{water} + E_{losses} \tag{2}$$

where the energy rate of the feed (E_{feed}) and the energy content of the air entering E_{air} define the input energy. While the energy rates of producer gas (E_{gas}), char (E_{char}), tar (E_{tar}), ash (E_{ash}), water (E_{water}), and losses in the gasifier E_{losses} represent the output of the gasifier system.

3.2.3 Exergy Balance

The current study also included an exergy analysis of gasification with lignite as a fuel. The system's thermodynamic performance is revealed through an exergy study. The gasification energy balance can be expressed as (Eq. (3)):

$$\sum \emptyset_{in} = \sum \emptyset_{out} + I \tag{3}$$

Where $\emptyset_{out}$ and $\emptyset_{in}$ are the output and input exergy, respectively, and I is the irreversibility that occurred during the conversion process. The change in enthalpy of a specific gas component from the reference state to the specified pressure and temperature is referred to as thermo-physical exergy. The normal chemical exergy mixing of all ingredients and the loss in entropy owing to the blending of different species of gases is referred to as the chemical exergy of the mixture. The ratio of the exergy of the producer gas to the sum of the exergy of the lignite and air is defined as exergy efficiency (Eq. (4)):

$$\eta_{ex} = \frac{\emptyset_{gas}}{\emptyset_{feed}} \tag{4}$$

1. Detailed procedures for calculating mass, energy, and exergy analysis can be found in the authors' previous work [6], [13], [14].

4. Results and Discussion

4.1 Temperature

Fig. 3 indicates the drying, pyrolysis, combustion, and reduction zone temperatures for different feedstock. The temperatures range in pyrolysis and the drying zone were observed between 355°C-452°C and 150°C-178°C, respectively. Moreover, the temperatures range in reduction and the combustion zone were observed between 570°C-675°C and 840°C-973°C, respectively. It was observed that the temperature was found higher when dolomite was added with feedstock. The thermal decomposition of dolomite is an endothermic process; however, thermal energy used by dolomite catalyst was released afterwards and boosted the Water Gas Shift reaction [15]. It is responsible for increasing the temperature in the combustion zone. It was also determined that wood feedstock offered higher temperatures than lignite feedstock. It may be because the wood has higher volatile matters and lower moisture–ash contents which would help to boost the temperature.
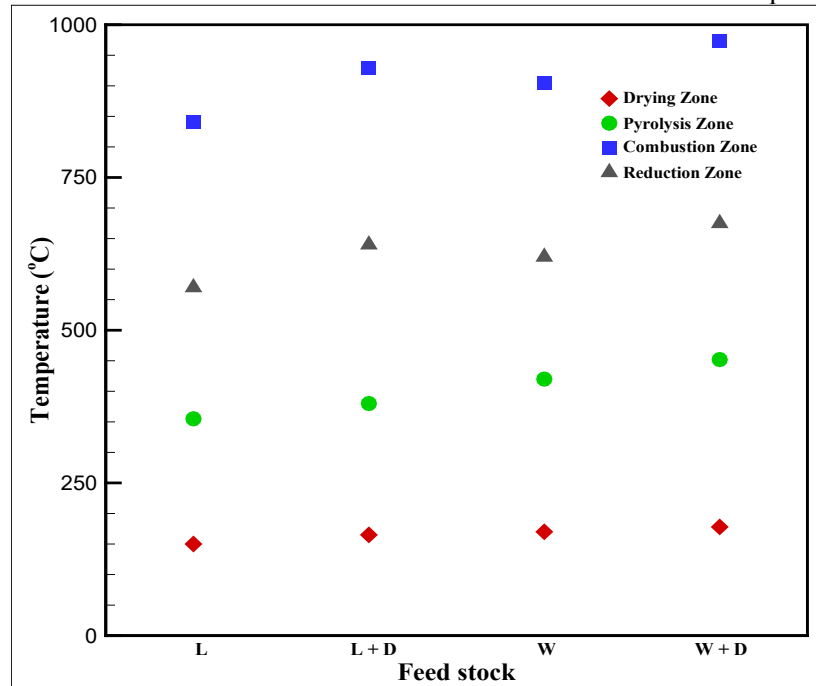

Fig. 3. Zone temperatures of different feedstock

Clinker formation was observed to be very common with lignite feedstock. Due to the same, the gasifier couldn't operate for a long time. It was found that after the addition of catalyst in the lignite, no clinkers were found during the 180 minutes of the experimental run. For wood feedstock also, no clinkers were observed.

4.2   Fuel consumption rate and producer gas

Fig. 4 includes each feedstock's fuel consumption, specific fuel consumption, and gas flow rate. Fuel and catalyst were weighed and blended before experiments started. The remaining fuel inside the gasifier reactor was measured after 3 hours of experimentation. The weight of the catalyst was found to be the same before and after the experiment. For selected feedstock, it was observed that fuel consumption was found in the range of 10.01 kg h^{-1} to 11.56 kg h^{-1}. Adding the catalyst into feedstock increases the fuel consumption rate, as shown in Table 3. It may be due to the catalyst activity and rate of reactions [16]. The catalyst would boost the reaction rate in the gasifier reactor due to thermodynamically promoting the active phase [17]. The dolomite catalyst would also enhance conversion efficiency by offering a large reaction contact area, potentially leading to higher fuel consumption. By employing a catalyst with feedstock, carbon conversion efficiency improves, resulting in higher fuel consumption and gas flow rates.

As a result, heavy tar was converted into a gas, possibly increasing gas yields [18]. It's possible because the gas yield increases when a catalyst is fed to the feedstock. The specific fuel consumption (SFC) was evaluated, as mentioned by Karagiannidis [19]. SFC was calculated and found in the range of 1.79 kg kWh^{-1} - 1.92 kg kWh^{-1} for all selected feedstock, which is also in line with the literature [19]. Catalysts offer lower SFC, which shows their positive effect on the gasification system.

Airflow and gas flow rates were also found to be incremental when the catalyst was employed in the reactor. The same trend aligns with fuel consumption, as mentioned in Fig.4.
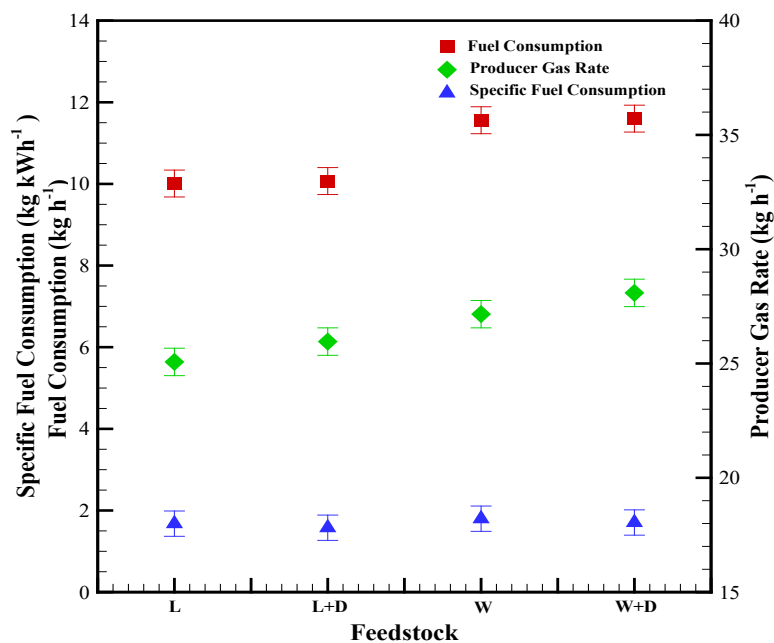

Fig. 4. Fuel consumption, specific fuel consumption, and gas flow rate of different feedstock

4.3   Gas composition and LHV of producer gas

The combustible gases, dust, soot, tar, particulates, and other non-combustible are present in the producer gas. The gasifier generates combustible gases, including CO, H_2, CH_4, and other hydrocarbons, as well as non-combustible gases, such as CO_2 and N_2. In contrast to H_2 and CO, the concentration of CH_4 in producer gas is substantially lower. Fig. 5 shows the concentrations of the producer gas compositions determined by gas chromatography, with lignite and wood as feedstock, total combustible gas content (CO, H_2, CH_4) 25.07% & 25.96% and 29.35% & 29.69% for with and without using a catalyst, respectively. The maximum combustible gas concentrations were observed with the addition of a catalyst in a feedstock. It is because the boudouard reaction occurred at higher temperatures and a favourable catalyst reactively at a higher temperature. With the use of catalysts, the concentration of CO and H_2 in the producer gas was found to be higher.

Furthermore, the tar reforming reaction on the catalyst surface was enhanced by the extraction of carbon, which resulted in the production of a wide range of CO and H_2 [20], [21]. With a catalyst, CO yield increased by 7.29% and 7.98%, respectively, when the catalyst was added to lignite and wood feedstock. The favourable Water Gas Shift (WGS) reaction at higher combustion zone temperatures resulted in a high H_2/CO in the producer gas [22]. It was observed that with a catalyst, the ratio of H_2/CO in the producing gas increased, as mentioned in Fig. 6. CO_2 concentrations decreased significantly when the experiment was carried out with a catalyst. However, the CH_4 content from all the feedstocks was almost constant.
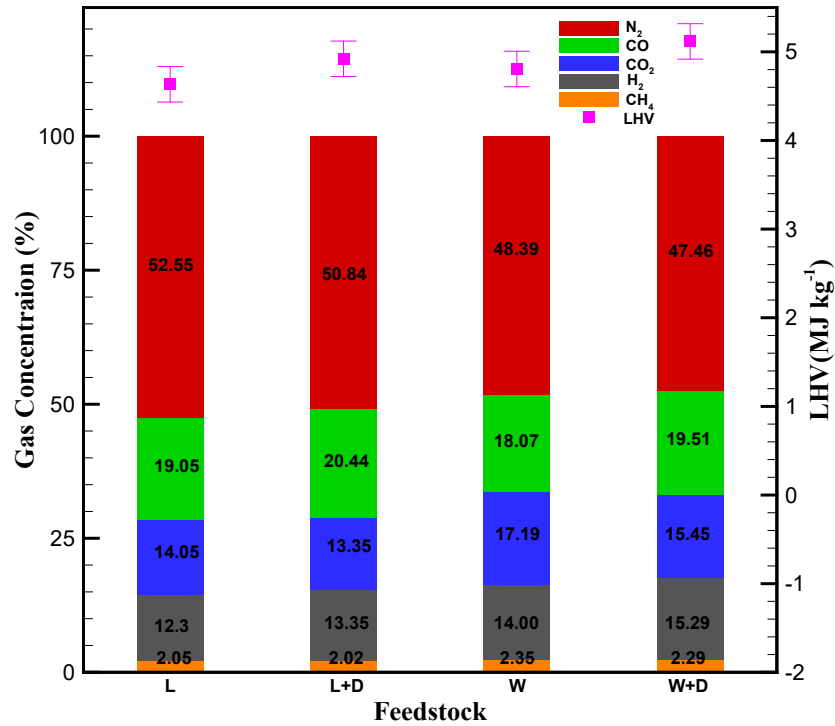
Fig. 5. Producer gas composition and LHV with different feedstock

Reed et al. [23] suggested a method for calculating the producer gas Lower Heating Value (LHV). For calculating the LHV of the producer gas, combustible constituents such as H_2, CO, and CH_4 gases were used. Heavy hydrocarbons were ignored due to their least significant compared to the other gases mentioned above. The LHV was calculated and found to be higher when fuel was blended with a dolomite catalyst, which is consistent with studies by Appell et al. [24]. It has a similar trend of H_2 and CO gases. The LHV remained between 4.63 and 5.11 MJ Nm^{-3} for all selected feedstock. The LHV of producer gas with different feedstock is shown in Fig. 5. The LHV was alleged in an incremental direction as dolomite was added in the lignite.
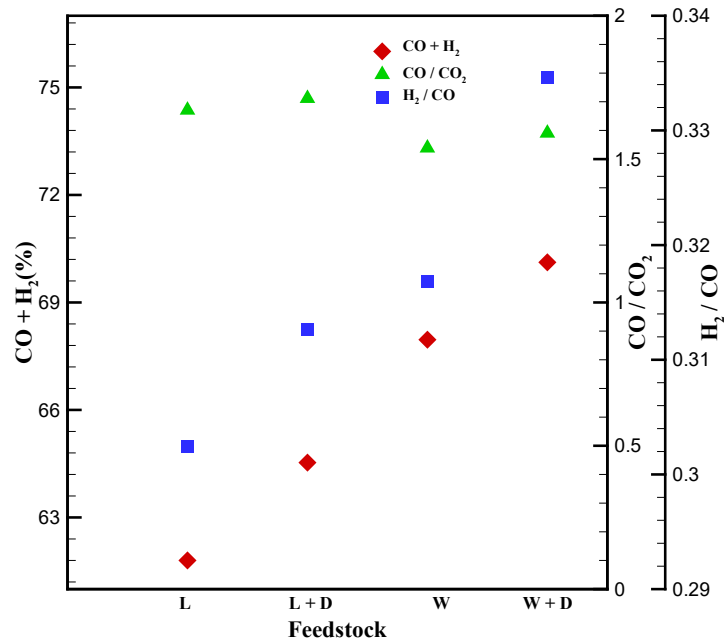
Fig. 6. Producer gas combustible constitutes and ratios with different feedstock

4.4 Mass balance

Table 3 shows the mass balance for various feeds and catalysts. In the gasification process, the mass of different feed and air mixes was used as an input, while the mass generated dry gas, char, water, and ash was used as an output. Because of its low concentration compared to other constituents in the output, the bulk of tar content in producer gas is usually overlooked. A hydrometer was used to assess the total moisture present in the product gas with all feedstock. The ash pit was used to collect ash and char. The amount of ash in the output was solely affected by the volume of fuel used. The char content was computed as a result of this. Because of the higher reaction temperatures, the char content decreased with the addition of the catalyst. Depending on output mass versus input mass, the Mass Balance Closure (MBC) was computed and found to be in the range of 1.02-1.04. The variability in MBC could be attributable to physical or measurement mistakes and uncertainty during the experiments.

Table 3. Mass Balance of different conditions.

Feed	Mass Input (kg h^{-1})			Mass Output (kg h^{-1})					MBC
	Fuel	Air	Total	Gas	Ash	Char	Water	Total	
L	10.01	17.07	27.08	25.07	1.24	0.24	1.09	27.64	1.021

L+D	10.07	17.26	27.33	25.96	1.32	0.2	0.95	28.43	1.040
W		11.56	17.79	29.35	27.16	0.60	1.09	1.39	30.24	1.030
W+D	11.6	18.09	29.69	28.09	0.63	1.05	1.23	31	1.044

4.5   Energy balance

Table 4 shows the input and output energies for various feedstock and the energy balance closure (EBC). Fuel energy is determined entirely by multiplying the LHV of fuel and the fuel consumption rate. Because the LHV per kg of feed remained constant, the energy rate of fuel is only dependent on fuel consumption. The airflow rate and temperature of air impact the energy of air. As multiple trials were conducted on different days, variations in air temperature were observed. The energy derived from ash was shown to be higher for lignite feedstock than wood feedstock due to the higher amount of ash content available in raw material. The trend of ash, char, and water in the energy balance is similar to the same mass balance for different feedstock. The ECB ratio was determined to be between 0.776 and 0.816.

Table 4. Energy balance of different conditions.

Energy Balance (MJ h^{-1})

Feed	Energy Input (MJ h^{-1})			Energy Output (MJ h^{-1})					EBC
	E_{Fuel}	E_{Air}	Total	E_{Gas}	E_{Ash}	E_{Char}	E_{Water}	Total	
L	163.864	0.171	164.034	132.986	0.074	0.401	0.333	133.794	0.816
L+D	164.846	0.173	165.019	137.738	0.079	0.334	0.290	138.441	0.839

W	210.854	0.178	211.032	156.526	0.036	1.820	0.425	158.807	0.753
W+D	211.584	0.181	211.765	162.076	0.038	1.754	0.376	164.243	0.776

4.6 Cold gas efficiency and Exergy analysis

Fig. 7 shows cold gas efficiency and exergy efficiency for various feedstock. Both the terms are measured as mentioned in literature [6], [25], [26]. It is observed that the addition of catalysts would be favourable in terms of cold gas efficiency and exergy efficiency. It may be due to the catalyst's higher fuel conversion efficiency and reactivity. Lignite offered higher cold gas efficiency compared to wood. It is because lignite had lower fuel consumption and offered relatively good quality producer gas.

Exergy analysis was carried out as mentioned in section 3.2. The composition of the fuel determines exergy. Because the exergy of fuel is independent of the fuel composition and stayed relatively stable throughout the experimental run, the exergy was increased with different feedstock. It can be observed from Fig. 7 that the exergy efficiency keeps on increasing with the catalyst. Exergy efficiency was calculated and found in the 56.10% – 64.92% range for selected feedstock.
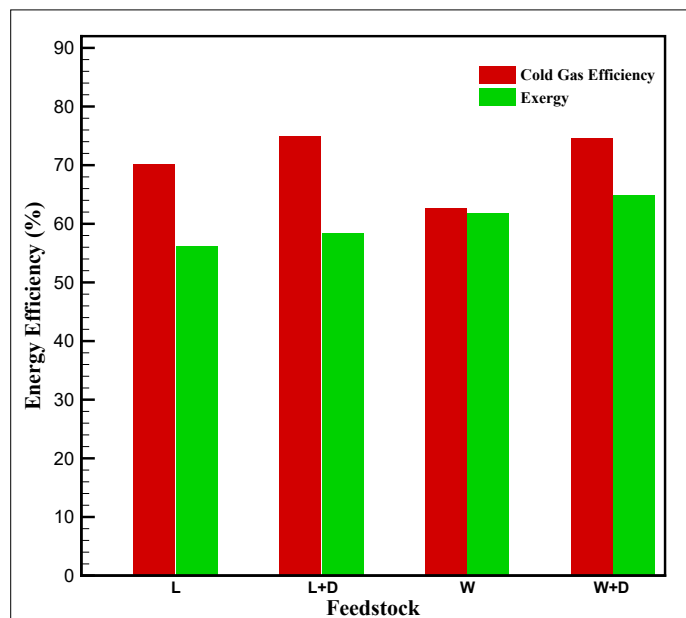

Fig .7. Cold gas efficiency and exergy efficiency for different feedstock

4.7 PM and tar in the producer gas

The PM and tar content harm the downstream gasifier process equipment in the producer gas. For gas turbines and internal combustion engines, experts have established a tolerable range for tar and PM [28] [29]. The PM was measured after the proper cleaning, while tar was measured from the gasifier system at two points: 1) just after the gasifier reactor and 2) after the cleaning system (before the gas burner). Fig. 8 depicts the amount of PM and tar in producer gas.
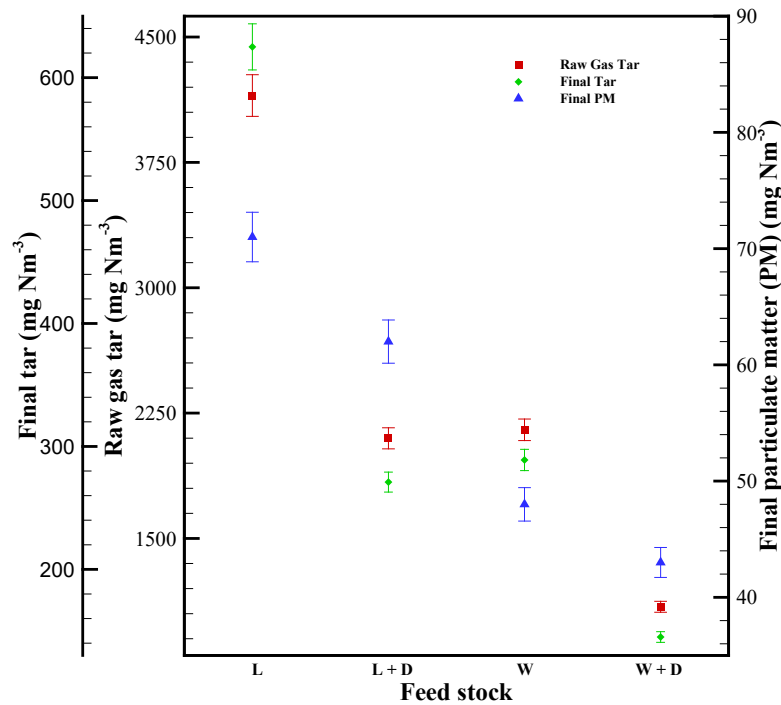
Fig. 8. PM and tar in the producer gas for different feedstock

PM concentrations were measured after the cleaning system (before the burner) and found to be between 48.11 and 71.12 mg Nm^{-3}. The use of a catalyst was shown to result in decreased PM levels in the producing gas. It's because, in the presence of a catalyst, a more significant temperature would transform huge PM into small particles. The concentrations of tar in producer gas immediately after the gasifier reactor and after the cleaning system were measured and found in the range of 1091 mg Nm^{-3}- 4150 mg Nm^{-3} and 145 mg Nm^{-3}- 625 mg Nm^{-3} for all selected (lignite and wood) feedstock. The dolomite played a significant role in destroying the tar in the producer gas. Reduction in tar is mainly due to catalyst activities inside the reactor and higher temperatures. Reduction in tar concentrations may increase the amount of combustible gases, improving the gasifier's overall performance. It was also observed that almost 85%-87% of tar is captured in the cleaning system compared to tar in raw gas measured immediately after the gasifier reactor.

5   Conclusions:

Experiments were conducted with two feedstocks (lignite and wood feedstock) and a catalyst to check its feasibility and performance on a 10 kWe downdraft gasifier. Lump dolomite was used as a catalyst (5%, W/W). The employment of a catalyst was responsible for all zone temperatures for both fuels. The CO and H_2 gas concentration was increased, whereas the CO_2 gas concentration was decreased for catalytic gasification. The CH_4 gas concentration was found to be almost constant. The fuel consumption, gas flow rate, and LHV of producer gas increased, whereas SFC decreased with the addition of a catalyst with fuels. Cold gas efficiency and exergy efficiency were calculated and found in the range of 62.60%-74.93% and 56.1%-64.9%. Mass balance closure (MBC) and Energy balance closure (EBC) were found in the range of 1.02 – 1.04 and 0.75 – 0.83, respectively for selected feedstock. 56.64% (L) and 49.83% (W) tar and 12.68% (L) and 10.42% (W) PM in the producer gas (collected after the cleaning system) were reduced when the catalyst was added in lignite and wood fuels, respectively. The major conclusion of this study is that adding a dolomite catalyst in lignite/wood feedstock improves the overall performance of the gasifier.

Acknowledgement:

from Science and Engineering Research Board to (Govt. of India) attend the 10th International Conference of Fluid Flow, Heat and Mass Transfer, Canada on 07 June 2023 to 09 June 2023.

Disclosure statement

No potential conflict of interest was reported by the authors.

References

[1] J. Phillips, "Different Types of Gasifi ers and Their Integration with Gas Turbines 1.2.1-1 Introduction," *Transport*, pp. 67–77, 2004.

[2] V. R. Patel, D. S. Upadhyay, and R. N. Patel, "Gasification of lignite in a fixed bed reactor: Influence of particle size on performance of downdraft gasifier," *Energy*, vol. 78, pp. 323–332, 2014, doi: 10.1016/j.energy.2014.10.017.

[3] D. S. Upadhyay, A. K. V Sakhiya, K. R. Panchal, and R. N. Patel, "Journal of Energy and Environmental Sustainability Thermodynamic Analysis of Lignite Gasification in the Downdraft Gasifier," pp. 58–64, 2018.

[4] V. R. Patel, D. Patel, N. S. Varia, and R. N. Patel, "Co-gasification of lignite and waste wood in a pilot-scale (10 kWe) downdraft gasifier," *Energy*, vol. 119, pp. 834–844, 2017, doi: 10.1016/j.energy.2016.11.057.

[5] H. Siddiqui, S. K. Thengane, S. Sharma, and S. M. Mahajani, "Revamping downdraft gasifier to minimize clinker formation for high-ash garden waste as feedstock," *Bioresour. Technol.*, vol. 266, pp. 220–231, Oct. 2018, doi: 10.1016/J.BIORTECH.2018.06.086.

[6] D. S. Upadhyay, A. Khosla, A. Chaudhary, and R. N. Patel, "Effect of catalyst to lignite ratio on the performance of a pilot scale fixed bed gasifier," *Energy*, vol. 189, 2019, doi: 10.1016/j.energy.2019.116229.

[7] H. V Makwana, D. S. Upadhyay, J. J. Barve, and R. N. Patel, "Strategies for Producer Gas Cleaning in Biomass Gasification : A Review," in *International Conference on Recent Advances in Bioenergy Research*, 2018, pp. 115–127.

[8] D. S. Upadhyay, H. V. Makwana, and R. N. Patel, "Performance evaluation of 10 kWe pilot scale downdraft gasifier with different feedstock," *J. Energy Inst.*, vol. 92, no. 4, pp. 913–922, 2019, doi: 10.1016/j.joei.2018.07.013.

[9] A. Chen, Z. Tian, R. Han, X. Wei, R. Hu, and Y. Chen, "Preparation of Ni-based steel slag catalyst by impregnation method for sludge steam gasification," *Sustain. Energy Technol. Assessments*, vol. 47, no. April, p. 101553, 2021, doi: 10.1016/j.seta.2021.101553.

[10] X. Zeng *et al.*, "Enhanced hydrogen production by the catalytic alkaline thermal gasification of cellulose with Ni/Fe dual-functional CaO based catalysts," *Int. J. Hydrogen Energy*, vol. 46, no. 65, pp. 32783–32799, 2021, doi: 10.1016/j.ijhydene.2021.07.142.

[11] Govt. of India, "Qualifying, Testing and Performance Evaluation of Biomass Gasifiers and Gasifier-Engine Systems, Gasifier Action Research," 2000.

[12] D. S. Upadhyay, K. R. Panchal, A. K. V. Sakhiya, and R. N. Patel, "Air-Steam gasification of lignite in a fixed bed gasifier: Influence of steam to lignite ratio on performance of downdraft gasifier," *Energy*, vol. 211, 2020, doi: 10.1016/j.energy.2020.118187.

[13] D. S. Upadhyay, A. K. V Sakhiya, K. R. Panchal, and R. N. Patel, "Thermodynamic Analysis of Lignite Gasification in the Downdraft Gasifier," *J. Energy Environ. Sustain.*, vol. 5, pp. 58–64, 2018.

[14] A. Kumar *et al.*, "Elemental and Heat Loss Analysis of Different Feedstock in Downdraft Gasifier," *J. Energy Environ. Sustain.*, vol. 7, pp. 10–16, 2019, doi: 10.47469/jees.2019.v07.100070.

[15] W. P. Walawender, D. A. Hoveland, and L. Fan, "Steam gasification of pure cellulose. 1. Uniform temperature profile," *Ind Eng Chem Process Des Dev*, vol. 24, pp. 813–817, 1985.

[16] Harald Jüntgen, "Application of catalysts to coal gasification processes. Incentives and perspectives," *Fuel*, vol. 62, no. 2, pp. 234–238, 1983.

[17] D. J.Marchand *et al.*, "Physical and chemical changes of coal during catalytic fluidized bed gasification," *Fuel Process. Technol.*, vol. 130, pp. 292–298, 2015.

[18] K. Kumabe, T. Hanaoka, S. Fujimoto, T. Minowa, and K. Sakanishi, "Co-gasification of woody biomass and coal with air and steam," *Fuel*, vol. 86, no. 5–6, pp. 684–689, 2007.

[19] K. Avraam, *opportunities and challenges for developing and transition economies.* .

[20] N. T. Thanasit Wongsiriamnuay, Nattakarn Kannang, "Effect of Operating Conditions on Catalytic Gasification of Bamboo in a Fluidized Bed," *Int. J. Chem. Eng.*, pp. 1–10, 2013.

[21] P. Basu, *Biomass Gasification and Pyrolysis: Practical Design and Theory*. Academic Press, Elsevier, 2010.

[22] Pfeifer P., "High-temperature/high-pressure water gas shift reaction to increase the H2/CO-ratio in syngas from biomass gasification."

[23] S. Technical *et al.*, *Handbook of Biomass Downdraft Gasifier Engine Systems*, no. March. SERI, 1988.

[24] H. Appell, I. Wender, and R. Miller, "Solubilization of Low Rank Coal With Carbon Monoxide and Water," *Chem. Ind.*, vol. 1703, 1969.

[25] K. Sandeep and S. Dasappa, "First and second law thermodynamic analysis of air and oxy-steam biomass gasification," *Int. J. Hydrogen Energy*, vol. 39, no. 34, pp. 19474–19484, 2014, doi: 10.1016/j.ijhydene.2014.09.134.

[26] D. S. Upadhyay, A. K. Sakhiya, K. Panchal, A. H. Patel, and R. N. Patel, "Effect of equivalence ratio on the performance of the downdraft gasifier – An experimental and modelling approach," *Energy*, vol. 168, pp. 833–846, 2019, doi: 10.1016/j.energy.2018.11.133.